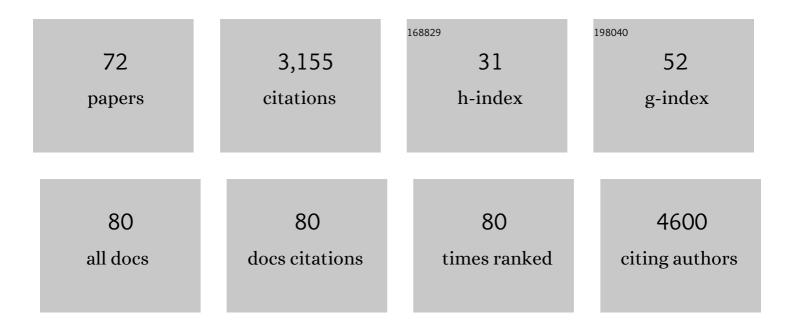
List of Publications by Year in descending order

Source: https://exaly.com/author-pdf/7014181/publications.pdf Version: 2024-02-01



#	Article	IF	CITATIONS
1	Coronaviral RNA-methyltransferases: function, structureÂand inhibition. Nucleic Acids Research, 2022, 50, 635-650.	6.5	35
2	Guanine quadruplexes in the RNA genome of the tick-borne encephalitis virus: their role as a new antiviral target andÂin virus biology. Nucleic Acids Research, 2022, 50, 4574-4600.	6.5	11
3	A Helquat-like Compound as a Potent Inhibitor of Flaviviral and Coronaviral Polymerases. Molecules, 2022, 27, 1894.	1.7	3
4	Discovery of isonucleotidic CDNs as potent STING agonists with immunomodulatory potential. Structure, 2022, 30, 1146-1156.e11.	1.6	9
5	Conformational ensemble of the full-length SARS-CoV-2 nucleocapsid (N) protein based on molecular simulations and SAXS data. Biophysical Chemistry, 2022, 288, 106843.	1.5	11
6	Structural basis for SARS-CoV-2 nucleocapsid (N) protein recognition by 14-3-3 proteins. Journal of Structural Biology, 2022, 214, 107879.	1.3	4
7	Structure-based virtual screening and molecular dynamics simulation of SARS-CoV-2 Guanine-N7 methyltransferase (nsp14) for identifying antiviral inhibitors against COVID-19. Journal of Biomolecular Structure and Dynamics, 2021, 39, 4582-4593.	2.0	73
8	Protein–Ligand Interactions in the STING Binding Site Probed by Rationally Designed Single-Point Mutations: Experiment and Theory. Biochemistry, 2021, 60, 607-620.	1.2	15
9	Ligand Strain and Its Conformational Complexity Is a Major Factor in the Binding of Cyclic Dinucleotides to STING Protein. Angewandte Chemie - International Edition, 2021, 60, 10172-10178.	7.2	22
10	Ligand Strain and Its Conformational Complexity Is a Major Factor in the Binding of Cyclic Dinucleotides to STING Protein. Angewandte Chemie, 2021, 133, 10260-10266.	1.6	3
11	Antiviral Properties of the NSAID Drug Naproxen Targeting the Nucleoprotein of SARS-CoV-2 Coronavirus. Molecules, 2021, 26, 2593.	1.7	29
12	Synthesis and Biological Evaluation of Phosphoester and Phosphorothioate Prodrugs of STING Agonist 3′,3′-c-Di(2′F,2′dAMP). Journal of Medicinal Chemistry, 2021, 64, 7596-7616.	2.9	28
13	The Structure-Based Design of SARS-CoV-2 nsp14 Methyltransferase Ligands Yields Nanomolar Inhibitors. ACS Infectious Diseases, 2021, 7, 2214-2220.	1.8	57
14	High-Throughput Fluorescent Assay for Inhibitor Screening of Proteases from RNA Viruses. Molecules, 2021, 26, 3792.	1.7	11
15	Structural Analysis of the OC43 Coronavirus 2′-O-RNA Methyltransferase. Journal of Virology, 2021, 95, e0046321.	1.5	10
16	Localization of SARS-CoV-2 Capping Enzymes Revealed by an Antibody against the nsp10 Subunit. Viruses, 2021, 13, 1487.	1.5	12
17	Non-Nucleotide RNA-Dependent RNA Polymerase Inhibitor That Blocks SARS-CoV-2 Replication. Viruses, 2021, 13, 1585.	1.5	22
18	Reviewing Antiviral Research Against Viruses Causing Human Diseases - A Structure Guided Approach. Current Molecular Pharmacology, 2021, 14, .	0.7	1

#	Article	IF	CITATIONS
19	Substrate Specificity of SARS-CoV-2 Nsp10-Nsp16 Methyltransferase. Viruses, 2021, 13, 1722.	1.5	22
20	Structural Understanding of SARS-CoV-2 Drug Targets, Active Site Contour Map Analysis and COVID-19 Therapeutics. Current Molecular Pharmacology, 2021, 14, .	0.7	4
21	Antiviral Activity of 7-Substituted 7-Deazapurine Ribonucleosides, Monophosphate Prodrugs, and Triphoshates against Emerging RNA Viruses. ACS Infectious Diseases, 2021, 7, 471-478.	1.8	22
22	Osh6 Revisited: Control of PS Transport by the Concerted Actions of PI4P and Sac1 Phosphatase. Frontiers in Molecular Biosciences, 2021, 8, 747601.	1.6	8
23	Enzymatic Synthesis of 3′–5′, 3′–5′ Cyclic Dinucleotides, Their Binding Properties to the Stimulato Interferon Genes Adaptor Protein, and Structure/Activity Correlations. Biochemistry, 2021, 60, 3714-3727.	or of 1.2	8
24	PI(3,4)P2-mediated cytokinetic abscission prevents early senescence and cataract formation. Science, 2021, 374, eabk0410.	6.0	37
25	Structural basis for hijacking of the host ACBD3 protein by bovine and porcine enteroviruses and kobuviruses. Archives of Virology, 2020, 165, 355-366.	0.9	7
26	Remdesivir triphosphate can efficiently inhibit the RNA-dependent RNA polymerase from various flaviviruses. Antiviral Research, 2020, 182, 104899.	1.9	40
27	Structural analysis of the SARS-CoV-2 methyltransferase complex involved in RNA cap creation bound to sinefungin. Nature Communications, 2020, 11, 3717.	5.8	226
28	Defining the subcellular distribution and metabolic channeling of phosphatidylinositol. Journal of Cell Biology, 2020, 219, .	2.3	57
29	Structural analysis of the putative SARS-CoV-2 primase complex. Journal of Structural Biology, 2020, 211, 107548.	1.3	61
30	Structural basis of RNA recognition by the SARS-CoV-2 nucleocapsid phosphoprotein. PLoS Pathogens, 2020, 16, e1009100.	2.1	206
31	Antiviral Drug Targets of Single-Stranded RNA Viruses Causing Chronic Human Diseases. Current Drug Targets, 2020, 21, 105-124.	1.0	18
32	Convergent evolution in the mechanisms of ACBD3 recruitment to picornavirus replication sites. PLoS Pathogens, 2019, 15, e1007962.	2.1	26
33	Structures of kobuviral and siciniviral polymerases reveal conserved mechanism of picornaviral polymerase activation. Journal of Structural Biology, 2019, 208, 92-98.	1.3	4
34	Enzymatic Preparation of 2′–5′,3′–5′-Cyclic Dinucleotides, Their Binding Properties to Stimulator Interferon Genes Adaptor Protein, and Structure/Activity Correlations. Journal of Medicinal Chemistry, 2019, 62, 10676-10690.	of 2.9	45
35	No magnesium is needed for binding of the stimulator of interferon genes to cyclic dinucleotides. Acta Crystallographica Section F, Structural Biology Communications, 2019, 75, 593-598.	0.4	14
36	A large scale high-throughput screen identifies chemical inhibitors of phosphatidylinositol 4-kinase type II alpha. Journal of Lipid Research, 2019, 60, 683-693.	2.0	16

#	Article	IF	CITATIONS
37	Phosphatidylinositol 4-kinase IIIβ (PI4KB) forms highly flexible heterocomplexes that include ACBD3, 14-3-3, and Rab11 proteins. Scientific Reports, 2019, 9, 567.	1.6	17
38	Structure of the yellow fever NS5 protein reveals conserved drug targets shared among flaviviruses. Antiviral Research, 2019, 169, 104536.	1.9	47
39	Structural insights into Acylâ€coenzyme A binding domain containing 3 (ACBD3) protein hijacking by picornaviruses. Protein Science, 2019, 28, 2073-2079.	3.1	7
40	PI(4,5)P2 controls plasma membrane PI4P and PS levels via ORP5/8 recruitment to ER–PM contact sites. Journal of Cell Biology, 2018, 217, 1797-1813.	2.3	153
41	The structural model of Zika virus RNA-dependent RNA polymerase in complex with RNA for rational design of novel nucleotide inhibitors. Scientific Reports, 2018, 8, 11132.	1.6	26
42	Structures of Dynamic Protein Complexes: Hybrid Techniques to Study MAP Kinase Complexes and the ESCRT System. Methods in Molecular Biology, 2018, 1688, 375-389.	0.4	9
43	Kobuviral Non-structural 3A Proteins Act as Molecular Harnesses to Hijack the Host ACBD3 Protein. Structure, 2017, 25, 219-230.	1.6	40
44	Adenosine triphosphate analogs can efficiently inhibit the Zika virus RNA-dependent RNA polymerase. Antiviral Research, 2017, 137, 131-133.	1.9	62
45	Metal ionsâ€binding T4 lysozyme as an intramolecular protein purification tag compatible with Xâ€ray crystallography. Protein Science, 2017, 26, 1116-1123.	3.1	7
46	Structural basis of Zika virus methyltransferase inhibition by sinefungin. Archives of Virology, 2017, 162, 2091-2096.	0.9	67
47	Rational Design of Novel Highly Potent and Selective Phosphatidylinositol 4-Kinase IIIβ (PI4KB) Inhibitors as Broad-Spectrum Antiviral Agents and Tools for Chemical Biology. Journal of Medicinal Chemistry, 2017, 60, 100-118.	2.9	50
48	Fluorescent Inhibitors as Tools To Characterize Enzymes: Case Study of the Lipid Kinase Phosphatidylinositol 4-Kinase IIIβ (PI4KB). Journal of Medicinal Chemistry, 2017, 60, 119-127.	2.9	19
49	Structural analysis of phosphatidylinositol 4-kinase IIIβ (PI4KB) – 14-3-3 protein complex reveals internal flexibility and explains 14-3-3 mediated protection from degradation in vitro. Journal of Structural Biology, 2017, 200, 36-44.	1.3	28
50	Negative charge and membrane-tethered viral 3B cooperate to recruit viral RNA dependent RNA polymerase 3D pol. Scientific Reports, 2017, 7, 17309.	1.6	18
51	Crystal structures of a yeast 14-3-3 protein from <i>Lachancea thermotolerans</i> in the unliganded form and bound to a human lipid kinase PI4KB-derived peptide reveal high evolutionary conservation. Acta Crystallographica Section F, Structural Biology Communications, 2016, 72, 799-803.	0.4	12
52	Structural insights and in vitro reconstitution of membrane targeting and activation of human PI4KB by the ACBD3 protein. Scientific Reports, 2016, 6, 23641.	1.6	81
53	Phosphatidylinositol 4-kinases: Function, structure, and inhibition. Experimental Cell Research, 2015, 337, 136-145.	1.2	123
54	Highly Selective Phosphatidylinositol 4-Kinase IIIβ Inhibitors and Structural Insight into Their Mode of Action. Journal of Medicinal Chemistry, 2015, 58, 3767-3793.	2.9	54

#	Article	IF	CITATIONS
55	The high-resolution crystal structure of phosphatidylinositol 4-kinase Ill ² and the crystal structure of phosphatidylinositol 4-kinase Ill ¹ ± containing a nucleoside analogue provide a structural basis for isoform-specific inhibitor design. Acta Crystallographica Section D: Biological Crystallography, 2015, 71, 1555-1563.	2.5	21
56	Norbornane-based nucleoside and nucleotide analogues locked in North conformation. Bioorganic and Medicinal Chemistry, 2015, 23, 184-191.	1.4	16
57	Large, dynamic, multi-protein complexes: a challenge for structural biology. Journal of Physics Condensed Matter, 2014, 26, 463103.	0.7	24
58	The crystal structure of the phosphatidylinositol 4â€kinase <scp>II</scp> α. EMBO Reports, 2014, 15, 1085-1092.	2.0	61
59	Endosomal sorting of VAMP3 is regulated by PI4K2A. Journal of Cell Science, 2014, 127, 3745-56.	1.2	50
60	Using cryoEM Reconstruction and Phase Extension to Determine Crystal Structure of Bacteriophage ϕ6 Major Capsid Protein. Protein Journal, 2013, 32, 635-640.	0.7	4
61	Subunit Folds and Maturation Pathway of a dsRNA Virus Capsid. Structure, 2013, 21, 1374-1383.	1.6	46
62	Membrane-Elasticity Model of Coatless Vesicle Budding Induced by ESCRT Complexes. PLoS Computational Biology, 2012, 8, e1002736.	1.5	44
63	Structural basis for membrane targeting by the MVB12-associated β-prism domain of the human ESCRT-I MVB12 subunit. Proceedings of the National Academy of Sciences of the United States of America, 2012, 109, 1901-1906.	3.3	49
64	Endosomal Sorting Complex Required for Transport (ESCRT) Complexes Induce Phase-separated Microdomains in Supported Lipid Bilayers. Journal of Biological Chemistry, 2012, 287, 28144-28151.	1.6	61
65	Solution Structure of the ESCRT-I and -II Supercomplex: Implications for Membrane Budding and Scission. Structure, 2012, 20, 874-886.	1.6	85
66	Solution structure of the ESCRT-I complex by small-angle X-ray scattering, EPR, and FRET spectroscopy. Proceedings of the National Academy of Sciences of the United States of America, 2011, 108, 9437-9442.	3.3	102
67	Structure of the human FOXO4-DBD–DNA complex at 1.9â€Ã resolution reveals new details of FOXO binding to the DNA. Acta Crystallographica Section D: Biological Crystallography, 2010, 66, 1351-1357.	2.5	54
68	14-3-3 protein interacts with and affects the structure of RGS domain of regulator of G protein signaling 3 (RGS3). Journal of Structural Biology, 2010, 170, 451-461.	1.3	34
69	Membrane Budding. Cell, 2010, 143, 875-887.	13.5	249
70	The 14-3-3 Protein Affects the Conformation of the Regulatory Domain of Human Tyrosine Hydroxylase. Biochemistry, 2008, 47, 1768-1777.	1.2	49
71	Both the N-terminal Loop and Wing W2 of the Forkhead Domain of Transcription Factor Foxo4 Are Important for DNA Binding. Journal of Biological Chemistry, 2007, 282, 8265-8275.	1.6	68
72	14-3-3 Protein Interacts with Nuclear Localization Sequence of Forkhead Transcription Factor FoxO4. Biochemistry, 2005, 44, 11608-11617.	1.2	100